INTERACTION OF A SPHERICAL ACOUSTIC WAVE WITH AN ELASTIC SPHERICAL SHELL

Gerald C. Lauchle

Pennsylvania State University

Prepared for:

Naval Sea Systems Command

6 March 1975

INTERACTION OF A SPHERICAL ACOUSTIC WAVE WITH AN ELASTIC SPHERICAL SHELL

Gerald C. Lauchle

Technical Memorandum
File No. TM 75-50
6 March 1975
Contract No. N00017-73-C-1418

Copy No. 28

The Pennsylvania State University
Institute for Science and Engineering
APPLIED RESEARCH LABORATORY
Post Office Box 30
State College, PA 16801

NAVY DEPARTMENT

NAVAL SEA SYSTEMS COMMAND

UNCLASSIFIED

SECURITY CLASSIFICATION OF THIS PAGE (When Data Entered)

REPORT DOCUMENTATION PAGE

READ INSTRUCTIONS BEFORE COMPLETING FORM

1. REPORT NUMBER: TM 75-50

2. GOVT ACCESSION NO.:

3. RECIPIENT'S CATALOG NUMBER:

4. TITLE (and Subtitle): INTERACTION OF A SPHERICAL ACOUSTIC WAVE WITH AN ELASTIC SPHERICAL SHELL

5. TYPE OF REPORT & PERIOD COVERED: Technical Memorandum

6. PERFORMING ORG. REPORT NUMBER:

7. AUTHOR(s): Gerald C. Lauchle

8. CONTRACT OR GRANT NUMBER(s): N00017-73-C-1418

9. PERFORMING ORGANIZATION NAME AND ADDRESS:
Applied Research Laboratory
P. O. Box 30
State College, PA 16801

10. PROGRAM ELEMENT, PROJECT, TASK AREA & WORK UNIT NUMBERS:

11. CONTROLLING OFFICE NAME AND ADDRESS:
Naval Sea Systems Command
Department of the Navy
Washington, DC 20362

12. REPORT DATE: 6 March 1975

13. NUMBER OF PAGES: 31

14. MONITORING AGENCY NAME & ADDRESS (if different from Controlling Office):

15. SECURITY CLASS. (of this report): Unclassified

15a. DECLASSIFICATION/DOWNGRADING SCHEDULE:

16. DISTRIBUTION STATEMENT (of this Report)

Approved for public release. Distribution unlimited.

Per NAVSEA - September 4, 1974

17. DISTRIBUTION STATEMENT (of the abstract entered in Block 20, if different from Report)

18. SUPPLEMENTARY NOTES

To be published in Journal of Sound and Vibration

19. KEY WORDS (Continue on reverse side if necessary and identify by block number)

Spherical shell;
Acoustic excitation;
Fluid loading;
Resonance response.

20. ABSTRACT (Continue on reverse side if necessary and identify by block number)

The interaction of a spherical acoustic wave with an elastic spherical shell is treated analytically. The solution includes the coupling between the acoustic sound field and vibration of the shell with any degree of fluid loading. The formulation for the far-field acoustic pressure is derived in terms of natural spherical wave functions, the properties of the acoustic medium, and the material constants of the shell. The far acoustic field is computed for a thin aluminum shell and several sound source locations over a large range of ka, where k is the wavenumber, and a is the shell radius.

DD FORM 1 JAN 73 1473 EDITION OF 1 NOV 65 IS OBSOLETE

PRICES SUBJECT TO CHANGE

UNCLASSIFIED

SECURITY CLASSIFICATION OF THIS PAGE (When Data Entered)

20. Abstract (Cont'd)

It is shown that the acoustic pressure depends significantly on whether the shell is in air or is submerged in water; particularly when the sound source is very near the surface. In air, the sound field of the shell is nearly identical to that of a rigid sphere but, in water, the shell is more compliant, which results in a damped radiation field that is characterized by vibrational resonances throughout the range of frequencies considered. As the sound source is moved further away from the surface, however, this resonance response decreases very rapidly, and the sound field corresponds more closely to that of the shell in air.

Abstract: The interaction of a spherical acoustic wave with an elastic spherical shell is treated analytically. The solution includes the coupling between the acoustic sound field and vibration of the shell with any degree of fluid loading. The formulation for the far-field acoustic pressure is derived in terms of natural spherical wave functions, the properties of the acoustic medium, and the material constants of the shell. The far acoustic field is computed for a thin aluminum shell and several sound source locations over a large range of ka, where k is the wavenumber, and a is the shell radius. It is shown that the acoustic pressure depends significantly on whether the shell is in air or is submerged in water; particularly when the sound source is very near the surface. In air, the sound field of the shell is nearly identical to that of a rigid sphere but, in water, the shell is more compliant, which results in a damped radiation field that is characterized by vibrational resonances throughout the range of frequencies considered. As the sound source is moved further away from the surface, however, this resonance response decreases very rapidly, and the sound field corresponds more closely to that of the shell in air.

---

*This memorandum contains a paper that has been submitted to the Journal of Sound and Vibration.

1. INTRODUCTION

In this paper the diffraction of a spherical sound wave by an elastic spherical shell of finite impedance is investigated analytically. It is assumed that the characteristic acoustic impedance of the medium is arbitrary relative to that of the shell material and that the radiation loading imposed by the medium may affect the vibration of the shell. It has been demonstrated by Maidanik and Kerwin [1], Crighton [2], King [3], Stuart [4], and others that both the finite mechanical impedance and fluid-loading effects can alter, significantly, the propagation of sound near simple membranes and plates. The results presented here essentially demonstrate the influence of these effects on the sound field generated by a spherical shell under the acoustic excitation of a simple monopole sound source. The sphere has been chosen to investigate these effects because of geometric symmetry, availability of an exact solution to the wave equation, and the fact that the mechanical impedance of a thin spherical shell can be derived in closed form.

Junger [5] has presented a formal normal-mode solution for the scattering of a plane wave by an elastic sphere, and in reference [6] he has investigated the point-excited spherical shell in an acoustic medium. The theory of point-excited spherical shells was further investigated by Hayek [7]. The analysis presented in this paper will follow the approach used by Junger [5], with the exception that the incident sound field is replaced by the free-space Green's function in spherical coordinates. The basic assumptions in the following analysis are: (1) the fluid medium is lossless; (2) the time dependence is harmonic ($e^{-i\omega t}$, where ω is the circular frequency); (3) the material of the shell is isotropic, has zero damping, and obeys

Hooke's law; (4) the shell is freely suspended; (5) the shearing strains are negligible; and (6) the thickness and deflections of the shell are much smaller than the radius a.

2. ANALYSIS

Figure 1 shows a sketch of a spherical shell of radius a and thickness 2h. The material of the shell has a mass density ρ_s, Young's modulus E, and Poisson's ratio μ; and, the acoustic medium has a mass density ρ and sound speed c. It is assumed that the monopole sound source is located on the axis of symmetry (z axis) at a distance r_o from the center of the sphere. The problem then reduces to an axisymmetric one that is independent of ϕ, the rotational spherical coordinate. The field depends only on the field radius r and the aspect angle θ.

A rigorous derivation of the shell dynamics equations is found in Junger [5, 6], so it need not be repeated here. For completeness, however, the more important equations will be presented. The radial (w) and tangential (u) displacements of the shell are each written in the form of series of spherical surface harmonics:

$$w = \sum_{n=0}^{\infty} a_n P_n(\cos\theta) e^{-i\omega t} \tag{1}$$

$$u = -\sum_{n=1}^{\infty} b_n P_n^1(\cos\theta) e^{-i\omega t} \quad , \tag{2}$$

where $P_n(x)$ is the Legendre polynomial, and $P_n^1(x)$ is the associated Legendre function of the first order. The coefficients a_n and b_n are generalized

coordinates, and they can be determined through the solution of Lagrange's equations:

$$\frac{d}{dt}\left(\frac{\partial T}{\partial \dot{a}_n}\right) - \frac{\partial T}{\partial a_n} + \frac{\partial V}{\partial a_n} = Q_n \tag{3}$$

$$\frac{d}{dt}\left(\frac{\partial T}{\partial \dot{b}_n}\right) - \frac{\partial T}{\partial b_n} + \frac{\partial V}{\partial b_n} = 0 \qquad n > 0 \tag{4}$$

where T is the kinetic energy of the shell and V is the potential energy. Expressions for these may be found in Love [8]. The generalized force Q_n is determined from the integral of the pressure acting on the shell, i.e.,

$$Q_n = -2\pi a^2 \int_0^{\pi} (p_i + p_s)\Big|_{r=a} P_n(\cos\theta) \sin\theta \, d\theta \quad . \tag{5}$$

The incident pressure field is expressed in terms of the free-space Green's function in spherical coordinates, viz, Morse and Feshbach [9]:

$$p_i = -k^2 \rho c Q (4\pi)^{-1} \sum_{n=0}^{\infty} (2n+1) P_n(\cos\theta) \begin{cases} j_n(kr_o) h_n^{(1)}(kr) & r > r_o \\ h_n^{(1)}(kr_o) j_n(kr) & r < r_o \end{cases} , \tag{6}$$

where k is the wavenumber (ω/c), Q is the volume flow of the monopole, and j_n and $h_n^{(1)}$ are spherical Bessel and Hankel functions of the first kind, respectively. Here and in the remainder of this paper, the harmonic time dependence will be suppressed. The scattered field is expressed in the form:

$$p_s = \sum_{n=0}^{\infty} c_n P_n(\cos\theta) h_n^{(1)}(kr) \quad , \tag{7}$$

and equation (5) becomes

$$Q_n = -\frac{4\pi a^2}{2n+1}\left[c_n h_n^{(1)}(ka) - \frac{k^2 \rho c Q}{4\pi}(2n+1) h_n^{(1)}(kr_o) j_n(ka)\right] \tag{8}$$

Lagrange's equations (3) and (4) will have the same form as those of Junger [5], but with Q_n being replaced by equation (8), i.e.,

$$-\frac{8\pi a^2 h \rho_s \omega^2}{2n+1} a_n + \frac{8\pi E h}{(1-\mu)(2n+1)}\left[2a_n - (n+1)n b_n\right] = Q_n \tag{9}$$

$$-8\pi a^2 h \rho_s \omega^2 \frac{n(n+1)}{(2n+1)} b_n + \frac{8\pi E h}{(1-\mu)} \frac{n(n+1)}{(2n+1)}\left[-a_n + \frac{n(n+1) - (1-\mu)}{(1+\mu)} b_n\right] = 0 \tag{10}$$

The simultaneous solution of these two equations results in a_n and b_n in terms of c_n. We find that

$$\frac{Q_n}{a_n} = -\frac{8\pi h}{(2n+1)}\left\{a^2 \rho_s \omega^2 - \frac{E}{(1-\mu)}\left[2 - \frac{(1+\mu)}{1 - \frac{(1-\mu)}{n(n+1)}\left[\frac{a^2\omega^2\rho_s(1+\mu)}{E} + 1\right]}\right]\right\} \tag{11}$$

but, recalling that $Q_n/(-i\omega a_n)$ is a mechanical modal impedance (in a vacuum), we can write an expression for the modal mechanical impedance of a thin spherical shell:

$$Z_n = -i\frac{8\pi ha}{(2n+1)}\left\{kac\rho_s - \frac{E}{kac(1-\mu)}\left[2 - \frac{(1+\mu)}{1 - \frac{(1-\mu)}{n(n+1)}\left[\frac{k^2a^2c^2\rho_s(1+\mu)}{E} + 1\right]}\right]\right\} \quad (12)$$

The coefficient of the scattered partial wave c_n may now be determined through the application of the additional boundary condition:

$$\dot{w} = -\frac{i}{\omega\rho}\frac{\partial p}{\partial r}\bigg|_{r=a} \quad . \quad (13a)$$

In terms of the displacement,

$$w = \frac{1}{\omega^2\rho}\frac{\partial p}{\partial r}\bigg|_{r=a} \quad . \quad (13b)$$

where $p = p_i + p_s$ and $w = w_i + w_s$ with

$$p_i = -\frac{kQ}{4\pi c}\sum_{n=0}^{\infty}(2n+1)P_n(\cos\theta)h_n^{(1)}(kr_o)j_n'(ka) \quad , \quad (14)$$

$$w_s = (kc^2\rho)^{-1}\sum_{n=0}^{\infty}c_nP_n(\cos\theta)h_n^{(1)\prime}(ka) \quad . \quad (15)$$

The prime on the spherical radial functions denotes differentiation with respect to the argument. Substituting equations (14) and (15) into equation (13b) and making use of equation (1) and (11) results in

$$c_n = \frac{k^2 \rho c Q}{4\pi} (2n+1) h_n^{(1)}(kr_o) \left[\frac{j_n(ka) - i \dfrac{(2n+1)Z_n}{4\pi a^2 \rho c} j_n'(ka)}{h_n^{(1)}(ka) - i \dfrac{(2n+1)Z_n}{4\pi a^2 \rho c} h_n^{(1)'}(ka)} \right] , \qquad (16)$$

from which the normal displacment w and the scattered pressure p_s can be fully determined.

It is noted that $(2n+1)Z_n/4\pi a^2$, which may be interpreted as a modal mechanical impedance per unit area, is analytically the same as the impedance discussed by Junger [5, 6]. Fluid loading may then be accounted for by adding to this impedance a term representing the reaction of the fluid medium. This added term is the modal radiation impedance of a spherical vibrator defined in Junger [10]. The loaded impedance is thus written:

$$\left[\frac{(2n+1)Z_n}{4\pi a^2} \right]_{\text{loaded}} = \left[\frac{(2n+1)Z_n}{4\pi a^2} + i\rho c \frac{h_n^{(1)}(ka)}{h_n^{(1)'}(ka)} \right] . \qquad (17)$$

It is further noted that the scattered pressure from either rigid or soft (pressure release) spherical scatterers may be deduced from equation (16) by letting $Z_n \to \infty$ or 0, respectively. The rigid case will be discussed in the numerical results to follow.

3. NUMERICAL COMPUTATIONS

As discussed earlier, fluid loading and finite mechanical impedance have been shown to significantly change the propagation of sound near surfaces. The purpose of the following computations is to demonstrate the effect these

added conditions have on the far-field sound pressure relative to what occurs for a rigid sphere. The far-field solution is derived by letting

$$h_n^{(1)}(kr) \xrightarrow[r \to \infty]{} \frac{i^{-n-1}}{kr} e^{ikr} \tag{18}$$

in equation (7) and normalizing the total pressure to the sound field of the monopole in the absence of the spherical baffle, i.e.,

$$p_o = -\frac{ik\rho cQ}{4\pi r} e^{ikr} \quad , \quad (r >> a) \quad . \tag{19}$$

The resulting expression for the total normalized pressure field, with fluid loading taken into account, is thus:

$$\frac{p(r,\theta)}{p_o} = \sum_{n=0}^{\infty} (2n+1)(-i)^n P_n(\cos\theta) \left\{ j_n(kr_o) - h_n^{(1)}(kr_o) \cdot \left[\frac{j_n(ka) + j_n'(ka) \dfrac{h_n^{(1)}(ka)}{h_n^{(1)'}(ka)} - i \dfrac{z_n}{\rho c} j_n'(ka)}{2h_n^{(1)}(ka) - i \dfrac{z_n}{\rho c} h_n^{(1)'}(ka)} \right] \right\} \quad , \tag{20}$$

where $$z_n = (2n+1)Z_n/4\pi a^2 \quad .$$

The numerical evaluation of equation (20) was performed on an IBM 360/72 digital computer located on The Pennsylvania State University Campus. The

spherical Bessel functions were computed by downward recursion as discussed by Corbató and Uretsky [11]. Aluminum was chosen as the shell material with $2h/a = 7.8125 \times 10^{-3}$ and 2.3437×10^{-2}, and the source locations included $r_o/a = 1.0$, 1.125, and 2.0. The mediums considered were air and water under standard conditions. The reduced frequency ka varied between 0.01 and 80. Before proceeding with the numerical results, a discussion of the convergence of equation (20) is in order. The parameters $ka = 29$, $2h/a = 6.95 \times 10^{-3}$, $r_o/a = 1.0$, and $\theta = 10°$ were arbitrarily chosen for the air medium, and the value of the series for the real and the imaginary parts were expressed as a function of truncation index. The results of this "convergence check" are shown in Figures 2(a) and 2(b). The curves represent the value of the sum as a function of the number of terms summed. It is clearly seen that convergence has occurred for truncation indices greater than approximately 24. In general, it was found that convergence occurs for truncation indices slightly greater than [ka], which is to be expected because of the manner in which spherical Bessel functions approach zero for orders greater than the argument. In the remaining computations, the summations were terminated after [ka + 0.5ka] terms.

The magnitude of the far-field acoustic pressure is presented as a function of ka in Figures 3 through 7 for the back-scattered direction ($\theta = 0°$) and for various shell thicknesses and source locations. In these figures, the uniform broken-line curve represents the frequency response of an assumed rigid sphere ($Z_n \to \infty$). We see that for $ka \geq 2.0$, the shell in air may be considered rigid. Structural response is absent over much of the frequency range because the characteristic acoustic impedance of air is much less than the mechanical impedance of the shell. When submerged in water, however, the fluid impedance and the mechanical impedance are more

closely matched, and the shell is more compliant. The resulting sound field is seen to be considerably different from the field in air. The overall levels (mean line) in water are approximately a factor of two less than the levels in air because for source locations near the surface, the reflection factor is similar to that of an infinite plane. In air, the reflection factor is +1, and in water where the fluid and structural impedances are matched, this factor is approximately 1/2. Figure 5 shows the frequency-response curves for $r_o/a = 2.0$, where the difference in levels between air and water has diminished considerably. It is expected here that the sphere no longer appears planar to the sound source, and the simplified reflection factor of an infinite plane will predict an inaccurate result.

The frequency response of the shell in water is seen to be characterized by many structural resonances. Due to the membrane theory of shells, all of these resonances are "squeezed together" for $ka > 30$, which makes them difficult to identify; but between thirty and forty of these resonant peaks were noted for $0.01 \leq ka \leq 80$. This number of resonances is consistent with the findings of Hayek [7] who presents the natural frequencies of thin, submerged spherical shells for a wide range of 2h/a. The spherically symmetric vibration mode of a spherical shell (the breathing mode) occurs at an extremely high frequency because of the large strain energy required to deform the shell in this manner. The lowest expected frequency for a vibration mode that actually deforms the shell, then, is the $n = 2$ or 2-noded mode [7]. The large resonance response at $ka = 0.5$ ($2h/a = 7.8125 \times 10^{-3}$) or $ka = 1.0$ ($2h/a = 2.3437 \times 10^{-2}$) is attributed to this mode. Figure 8 shows the directivity function ($|p/p_o|$ vs. θ) for the thinner of the two shells considered at $ka = 0.5$. The shape of the directivity curve is quadrupole, which is the type expected for a sphere vibrating in a two-noded

mode. As r_o/a increases, the magnitude of this resonance decreases rapidly as depicted in Figures 3, 4, and 5. The response in both air and water is nearly identical for $r_o/a = 2.0$ (Figure 5), which indicates that the farfield does not depend very much on fluid-loading effects when the incident wave originates at distances greater than or comparable to the sphere radius. The inference may not generally apply to the finite impedance effect, however, because there may indeed be combinations of $2h/a$, E, ρ_s, etc., which make that effect important. This observation may be further explained by the reciprocity principle. The results for $r_o/a < 2.0$ essentially show the influence of fluid loading near the surface for plane wave incidence. It has been stressed by previous researchers that it is near the surface where the fluid-loading effects are most significant and where these computations support that hypothesis.

The curves of Figures 6 and 7 demonstrate that as the shell becomes thicker, the response in water is less affected by fluid-loading and structural-vibration effects, and begins to approach the response of the shell in air.

It is noted in Figures 3 through 7 that a periodicity is occurring in the frequency response for all source locations ($ka \gtrsim 5$). The period of these oscillations (in ka units) is approximately $\pi a/(r_o - a)$, which corresponds to the separation distance between source and surface of one-half wavelength. This indicates that the field is primarily due to specular reflection, and diffraction at the shadow boundary is of only secondary importance. As $r_o/a \to 2.0$, however, diffraction becomes more important, as indicated by the discrepancy in the predicted period of π and the observed period of approximately 3π.

The directivity functions in air and in water for an aluminum shell

with $2h/a = 7.8125 \times 10^{-3}$, $r_o/a = 1.125$, and $ka = 10.0$ are shown in Figure 9, and the phase angles relative to the incident sound field are shown as a function of θ in Figure 10. The relative change in phase angle between air and water is a measure of the degree of damping imposed by the heavy fluid medium. The directivity function for $ka = 25.0$ is shown in Figure 11.

4. SUMMARY

In this paper, the interaction of a spherical acoustic wave with an elastic spherical shell is treated analytically. The numerical results for a thin aluminum shell in water indicate that fluid-loading effects are most important in the far-field radiation when the distance between the source and the surface of the shell is less than the radius of the sphere. For these source locations, a strong resonance response was noted at a small value of ka. The far-field directivity function at this resonance frequency indicates that the sphere is vibrating in a 2-noded mode. The frequency response for the shell in water is characterized by many resonances over a wide frequency range, but their magnitude was considerably less than that for the 2-noded mode. In general, the far-field scattering of a spherical shell in air corresponds closely to that of a rigid sphere; whereas, in water, the field is influenced by resonant radiation and damping due to the compliance of the shell. The directivity functions for source locations near the surface were found to be typically omnidirectional for angles well into the shadow region but, for angles much greater than the shadow angle, wave interference becomes noticeable.

GCL:jdw
6 March 1975

ACKNOWLEDGMENTS

The author is grateful to Dr. S. I. Hayek and Dr. E. J. Skudrzyk for various discussions pertaining to this investigation. This effort was supported by the Applied Research Laboratory of The Pennsylvania State University under contract with the Naval Sea Systems Command.

GCL:jdw
6 March 1975

REFERENCES

1. G. Maidanik and E. M. Kerwin, Jr. 1966 Journal of the Acoustical Society of America 40, 1034-1038. Influence of fluid loading on the radiation from infinite plates below the critical frequency.

2. D. G. Crighton 1971 Journal of Fluid Mechanics 47, 625-638. Acoustic beaming and reflexion from wave-bearing surfaces.

3. W. F. King III 1973 Journal of Sound and Vibration 30, 279-288. The influence of fluid loading on acoustic propagation near surfaces.

4. A. D. Stuart 1972 PhD Dissertation, The Pennsylvania State University, University Park, Pennsylvania. Acoustic radiation from a point excited infinite elastic plate.

5. M. C. Junger 1952 Journal of the Acoustical Society of America 24, 366-373. Sound scattering by thin elastic shells.

6. M. C. Junger 1952 Journal of Applied Mechanics 19, 439-445. Vibrations of elastic shells in a fluid medium and the associated radiation of sound.

7. S. Hayek 1966 Journal of the Acoustical Society of America 40, 342-348. Vibration of a spherical shell in an acoustic medium.

8. A. E. H. Love 1944 A Treatise on the Mathematical Theory of Elasticity. New York: Dover Publications, fourth edition.

9. P. M. Morse and H. Feshbach 1953 Methods of Theoretical Physics (two volumes). New York: McGraw-Hill Book Company, Incorporated.

10. M. C. Junger 1952 Journal of the Acoustical Society of America 24, 288-289. Radiation loading of cylindrical and spherical surfaces.

11. F. J. Corbató and J. L. Uretsky 1959 Journal of the Association of Computing Machinery 6, 366-375. Generation of spherical Bessel functions in digital computers.

GCL:jdw
6 March 1975

FIGURE LEGEND

Figure 1. Sketch of the spherical shell in relation to the spherical and Cartesian coordinate systems.

Figure 2. Value of the modal series as a function of number of terms summed: (a) Real part, and (b) Imaginary part.

Figure 3. Frequency response of far-field acoustic pressure: Aluminum shell with $2h/a = 7.8125 \times 10^{-3}$, $r_o/a = 1.0$, ——— in air, —— - —— in water, and - - - - rigid.

Figure 4. Frequency response of far-field acoustic pressure: Aluminum shell with $2h/a = 7.8125 \times 10^{-3}$, $r_o/a = 1.125$, ——— in air, —— - —— in water, and - - - - rigid.

Figure 5. Frequency response of far-field acoustic pressure: Aluminum shell with $2h/a = 7.8125 \times 10^{-3}$, $r_o/a = 2.0$, ——— in air or rigid, and —— - —— in water.

Figure 6. Frequency response of far-field acoustic pressure: Aluminum shell with $2h/a = 2.3437 \times 10^{-2}$, $r_o/a = 1.0$, ——— in air, —— - —— in water, and - - - - rigid.

Figure 7. Frequency response of far-field acoustic pressure: Aluminum shell with $2h/a = 2.3437 \times 10^{-2}$, $r_o/a = 1.125$, ——— in air, —— - —— in water, and - - - - rigid.

Figure 8. Directivity functions for aluminum shell in water with $ka = 0.5$ and $2h/a = 7.8125 \times 10^{-3}$.

Figure 9. Directivity function for aluminum shell with $ka = 10.0$, $2h/a = 7.8125 \times 10^{-3}$, $r_o/a = 1.125$, ——— in air, and - - - - in water.

GCL:jdw
6 March 1975

Figure 10. Phase angle relative to incident field as a function of aspect angle for aluminum shell with ka = 10.0, $2h/a = 7.8125 \times 10^{-3}$, $r_o/a = 1.125$, ——— in air, and - - - - in water.

Figure 11. Directivity function for aluminum shell with ka = 25.0, $2h/a = 7.8125 \times 10^{-3}$, $r_o/a = 1.125$, ——— in air, and - - - - in water.

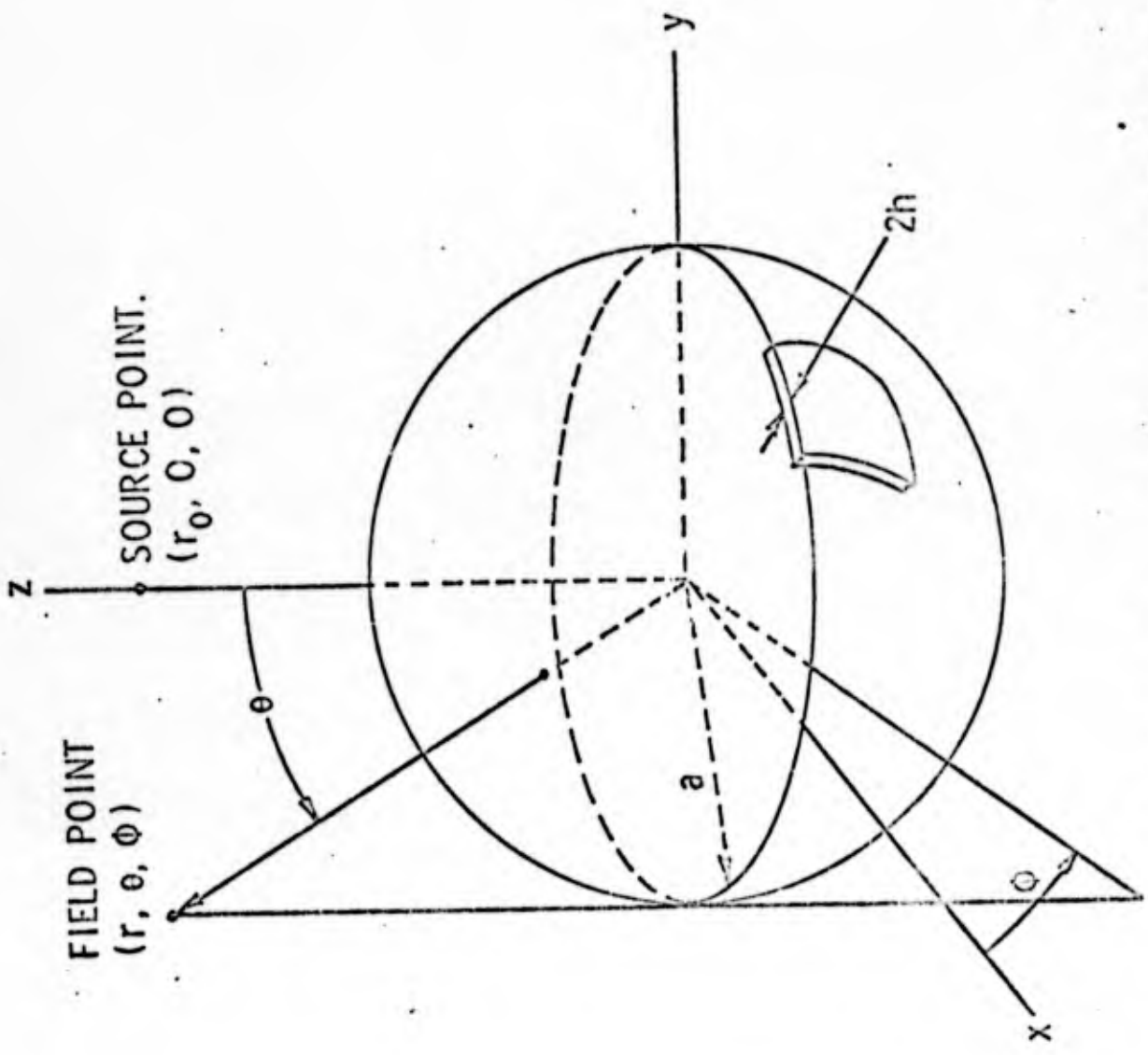

Fig. 1. Sketch of the spherical shell in relation to the spherical and Cartesian coordinate systems.

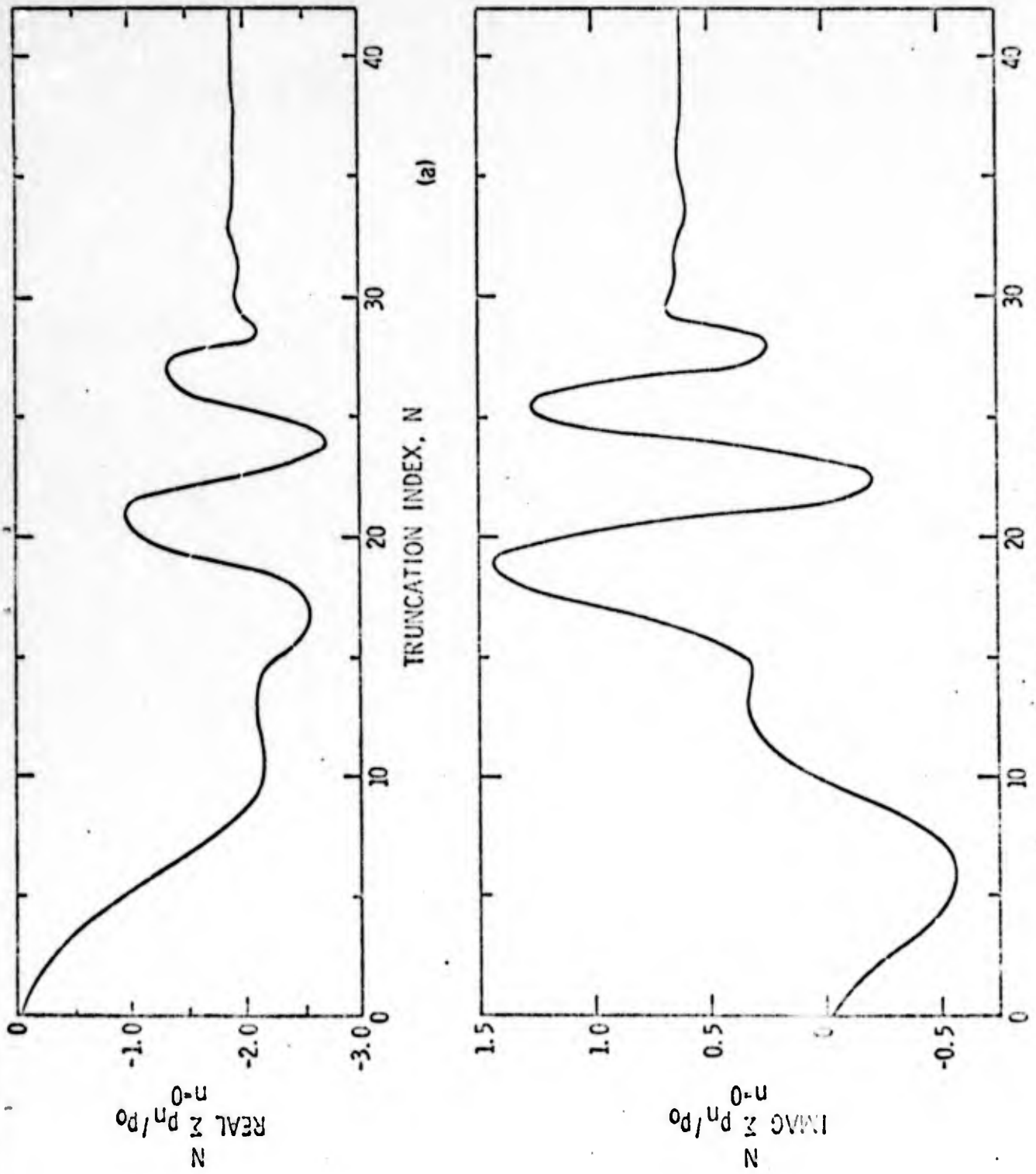

Fig. 2. Value of the modal series as a function of number of terms summed: (a) Real part, and (b) Imaginary part.

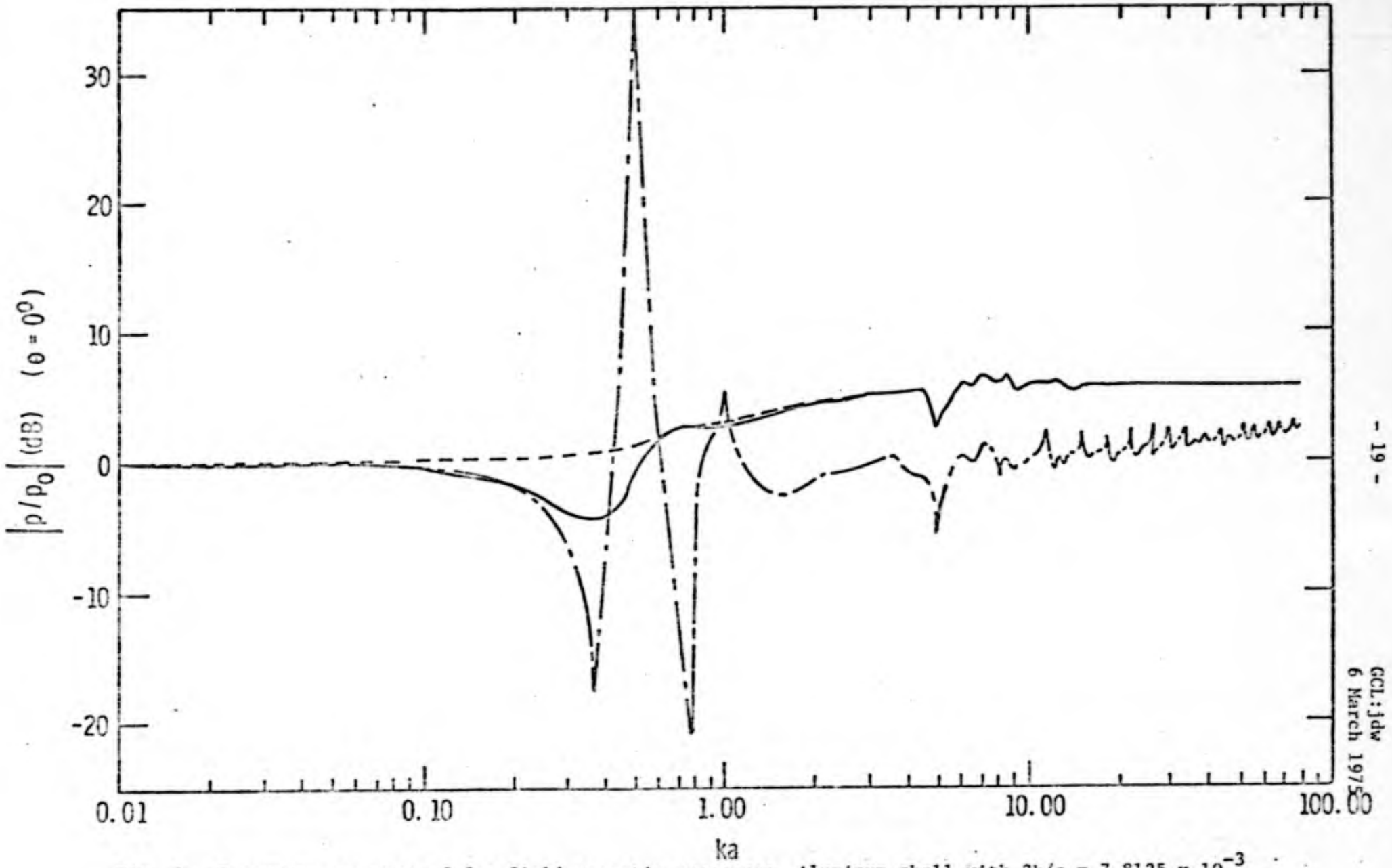

Fig. 3. Frequency response of far-field acoustic pressure: Aluminum shell with $2h/a = 7.8125 \times 10^{-3}$, $r_o/a = 1.0$, ——— in air, —— – —— in water, and - - - - rigid.

GCL:jdw
6 March 1975

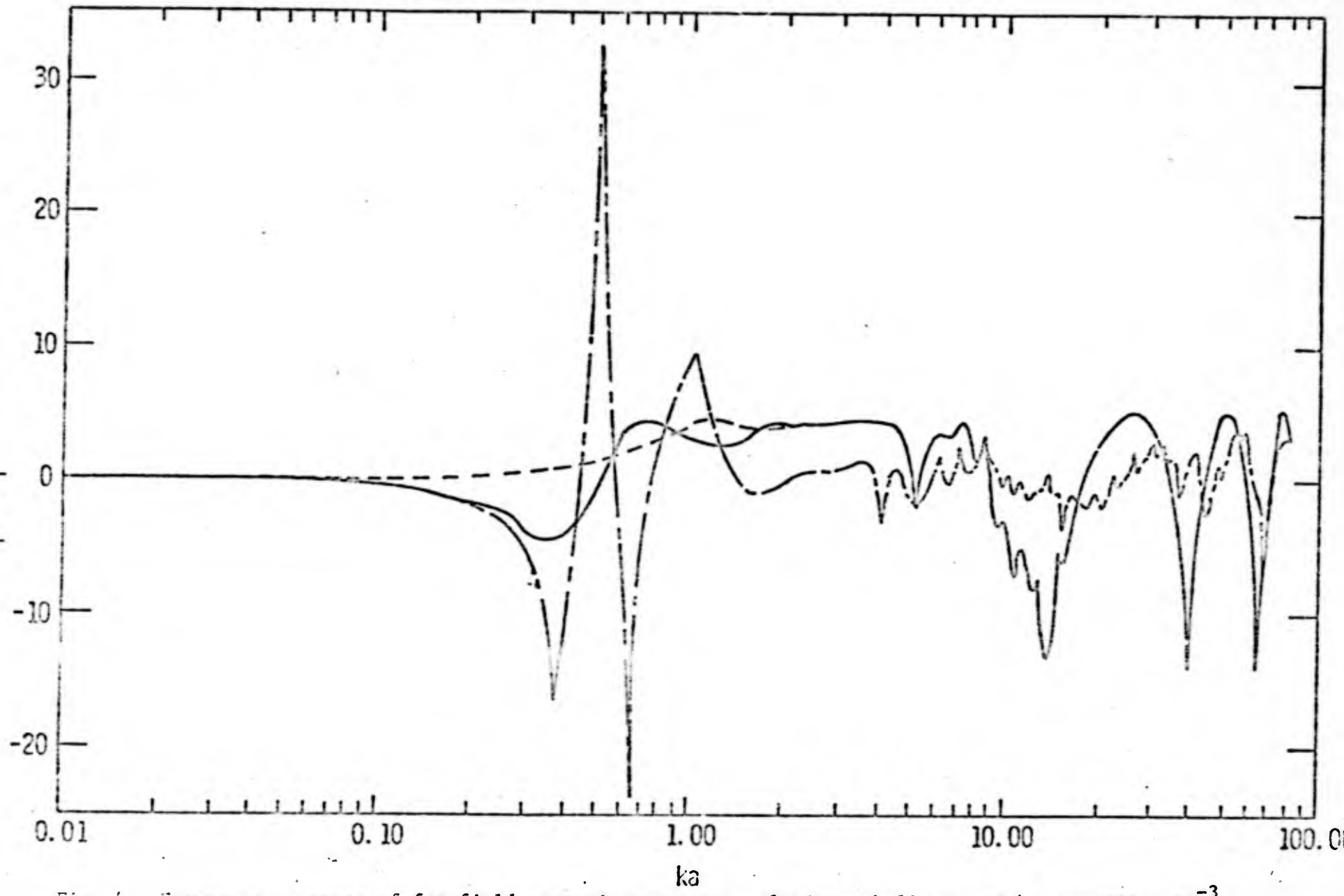

Fig. 4. Frequency response of far-field acoustic pressure: Aluminum shell with $2h/a = 7.8125 \times 10^{-3}$, $r_o/a = 1.125$, ——— in air, —— – —— in water, and -.- - - rigid.

GCL:jdw
6 March 1975

GCL:jdw
6 March 1975

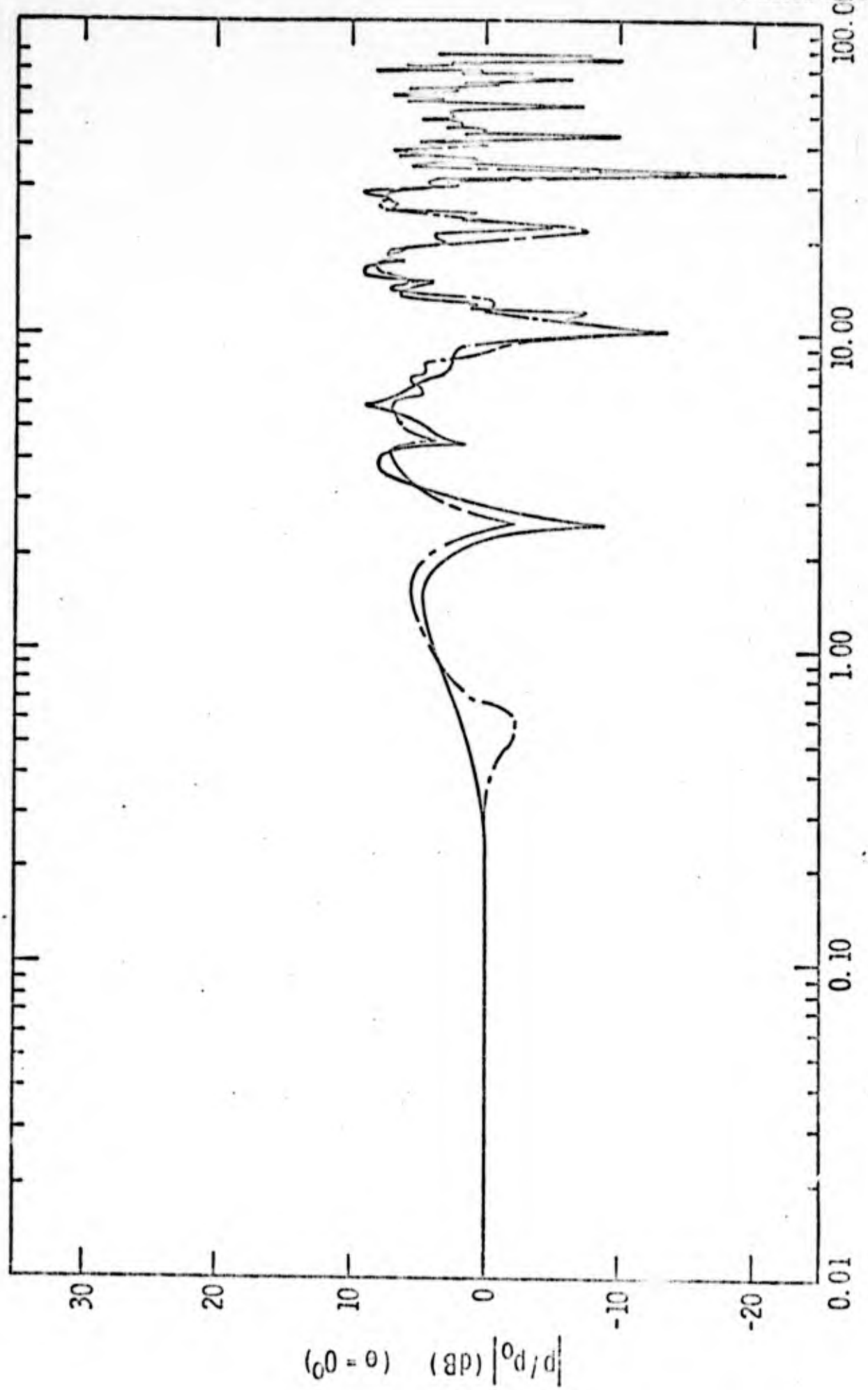

Fig. 5. Frequency response of far-field acoustic pressure: Aluminum shell with $2h/a = 7.8125 \times 10^{-3}$, $r_o/a = 2.0$, ——— in air or rigid, and — — — in water.

GCL:jdw
6 March 1975

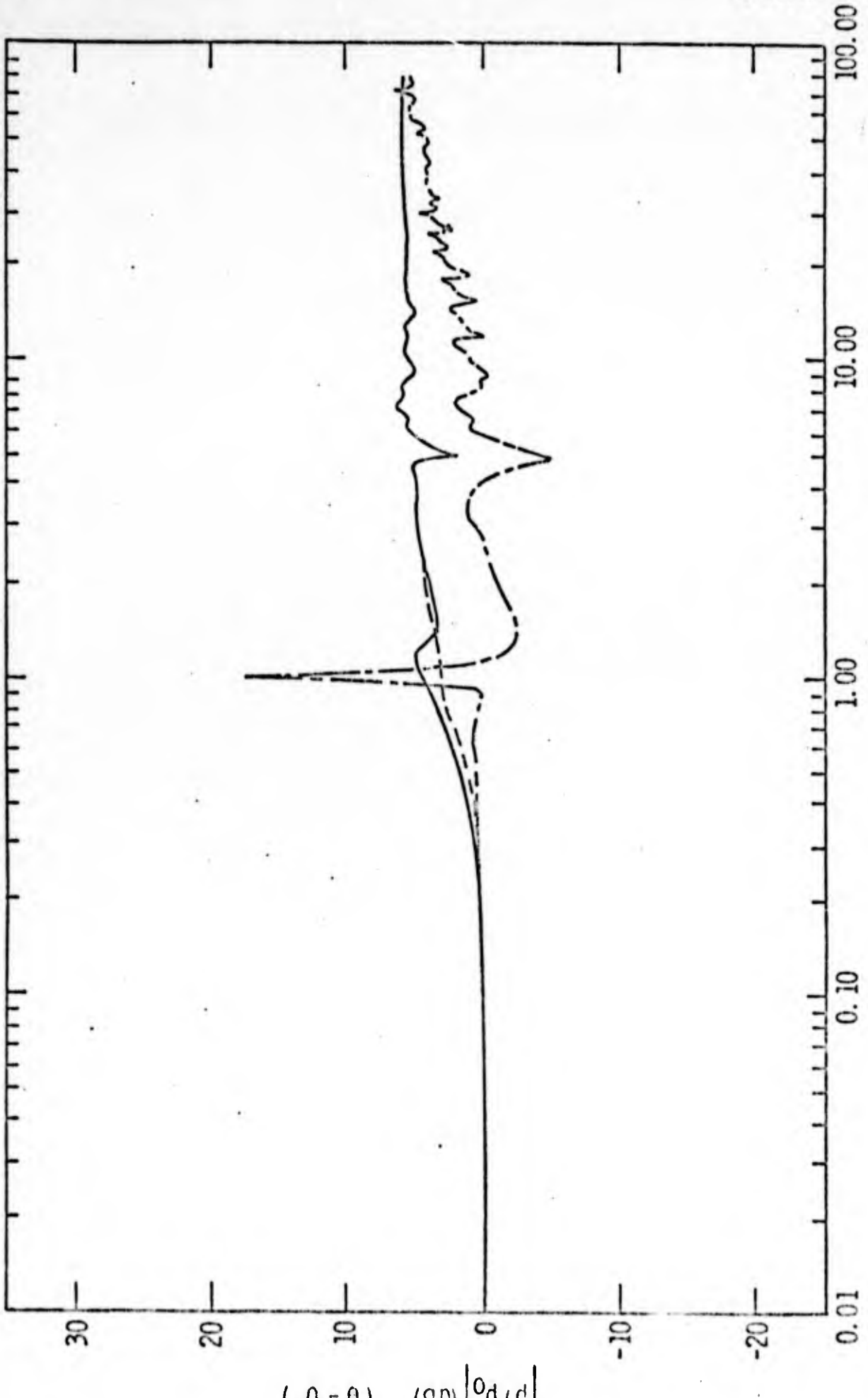

Fig. 6. Frequency response of far-field acoustic pressure: Aluminum shell with $2h/a = 2.3437 \times 10^{-2}$, $r_o/a = 1.0$, ——— in air, — — — — in water, and - - - - rigid.

CCL:jdw
6 March 1975

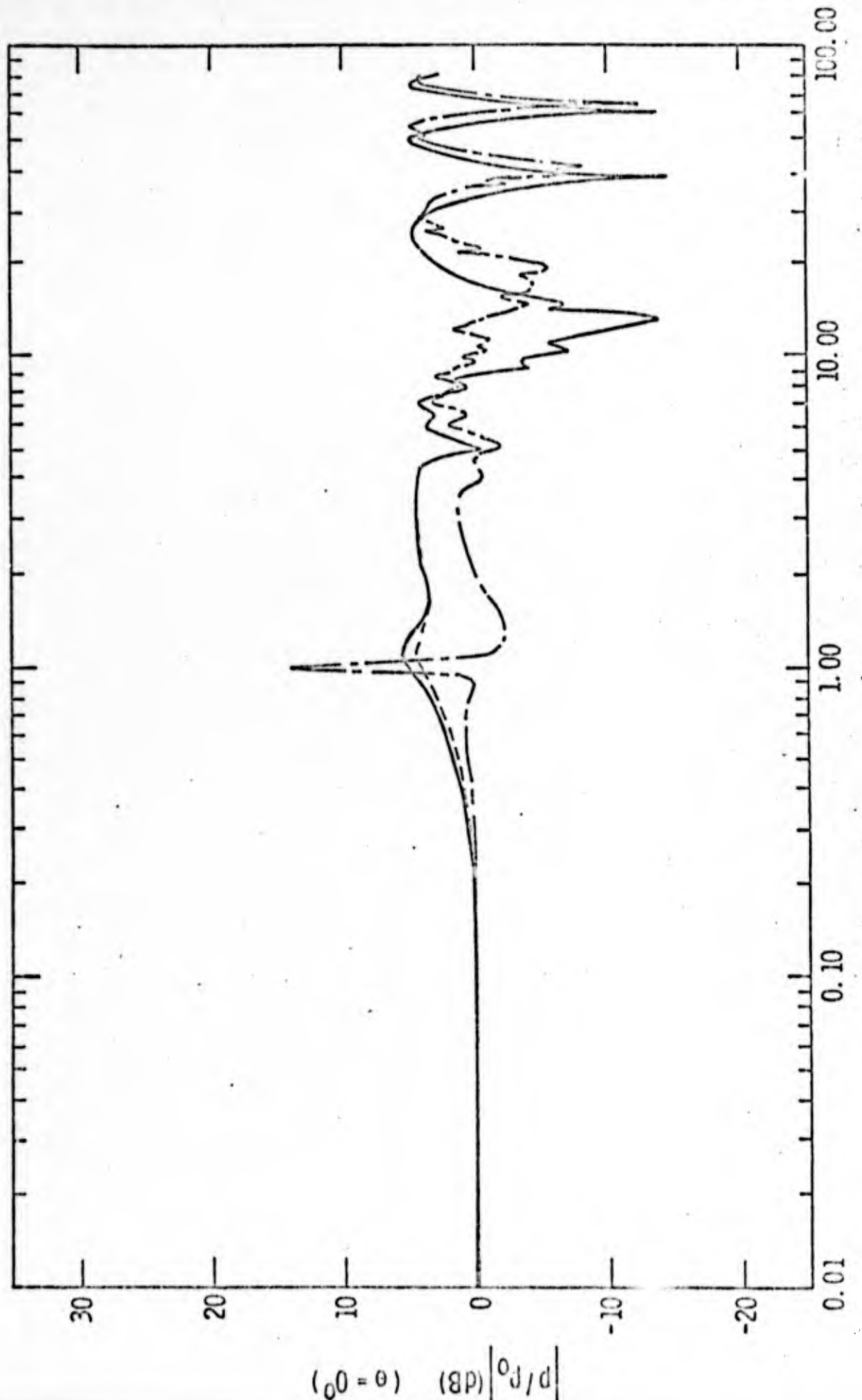

Fig. 7. Frequency response of far-field acoustic pressure: Aluminum shell with $2h/a = 2.3437 \times 10^{-2}$, $r_o/a = 1.125$, ——— in air, — — — in water, and - - - - rigid.

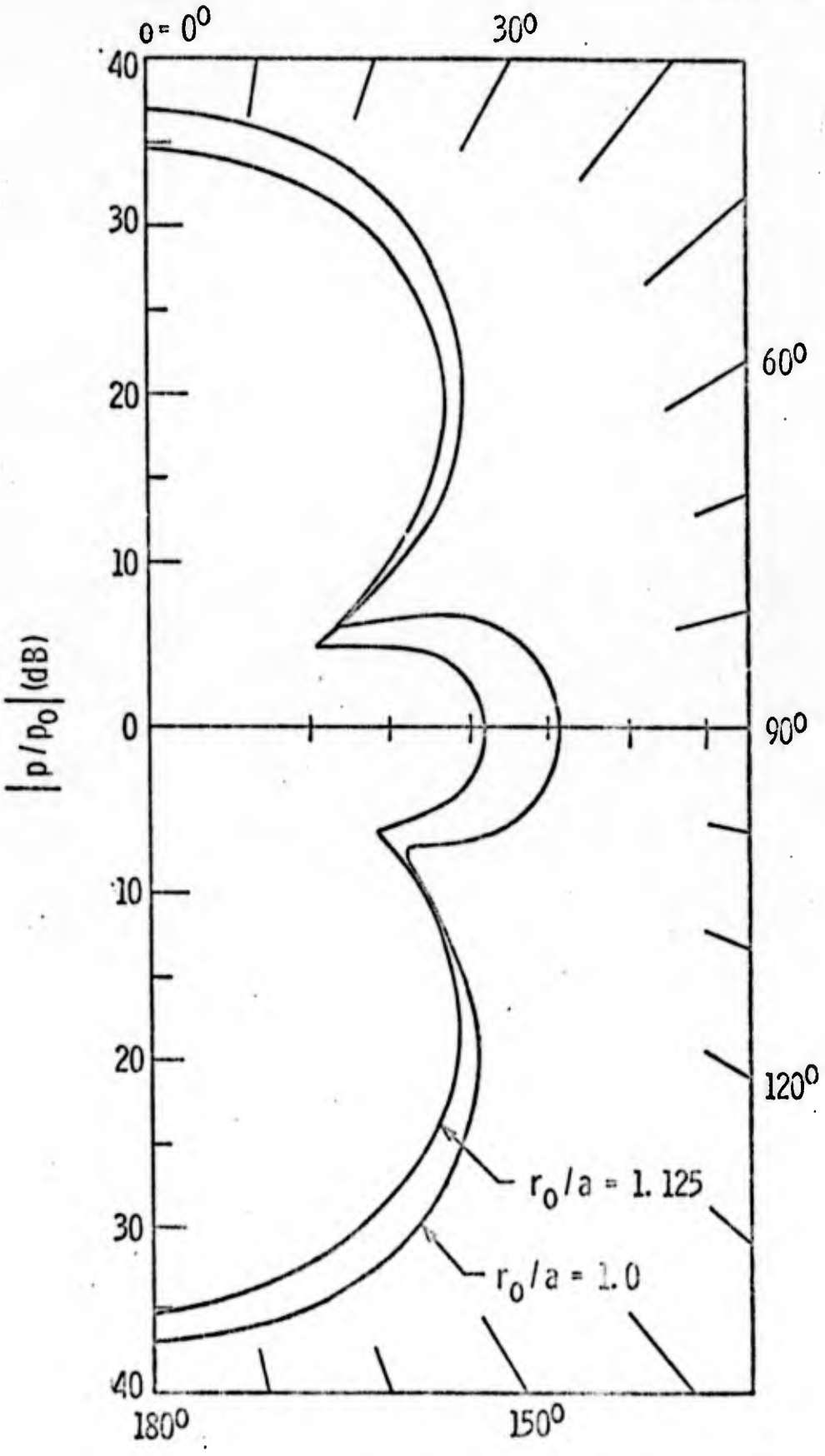

Fig. 8. Directivity function for aluminum shell in water with ka = 0.5 and 2h/a = 7.8125 x 10^{-3}.

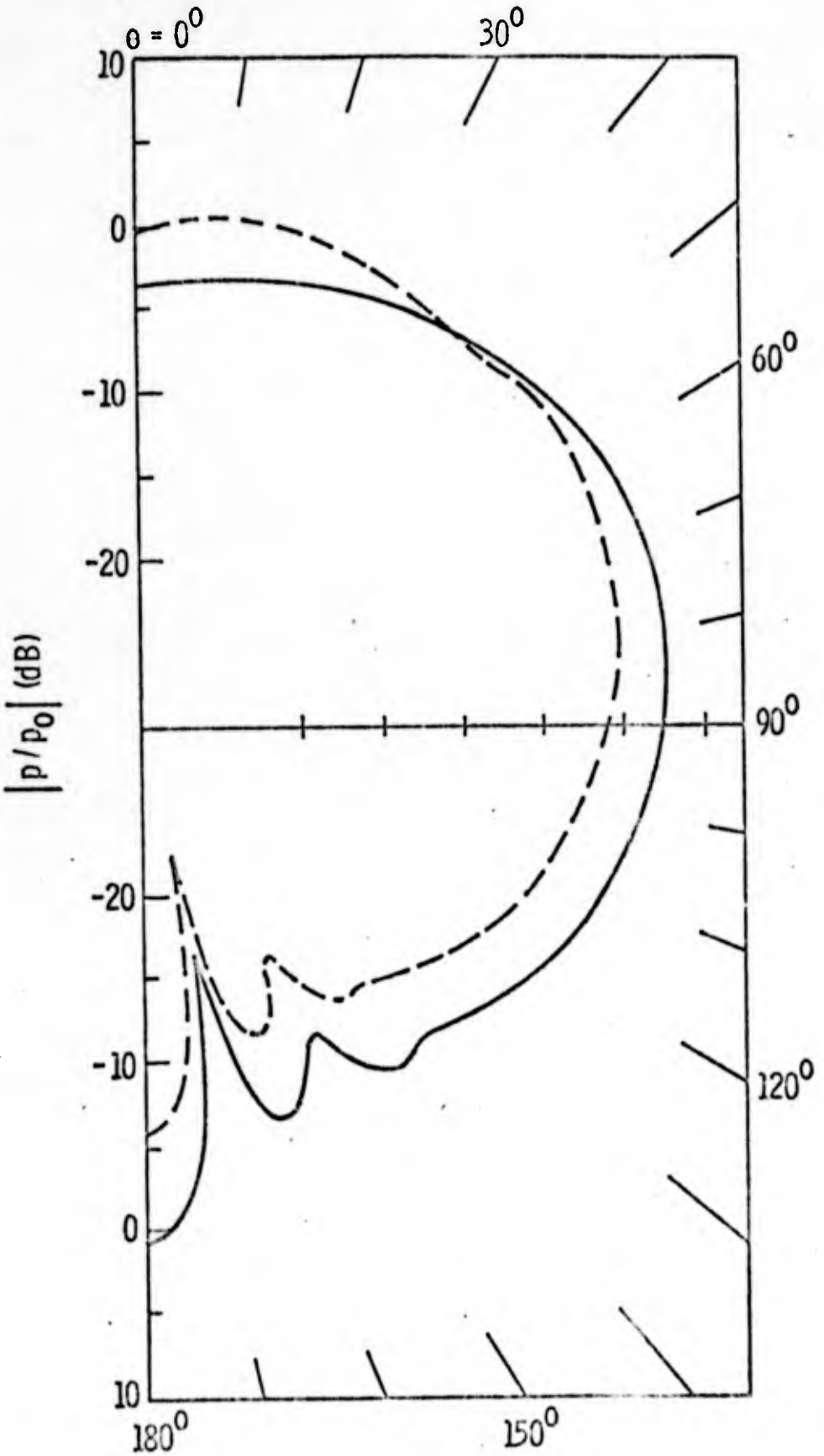

Fig. 9. Directivity function for aluminum shell with ka = 10.0, 2h/a = 7.8125 x 10^{-3}, r_0/a = 1.125, ——— in air, and - - - - in water.

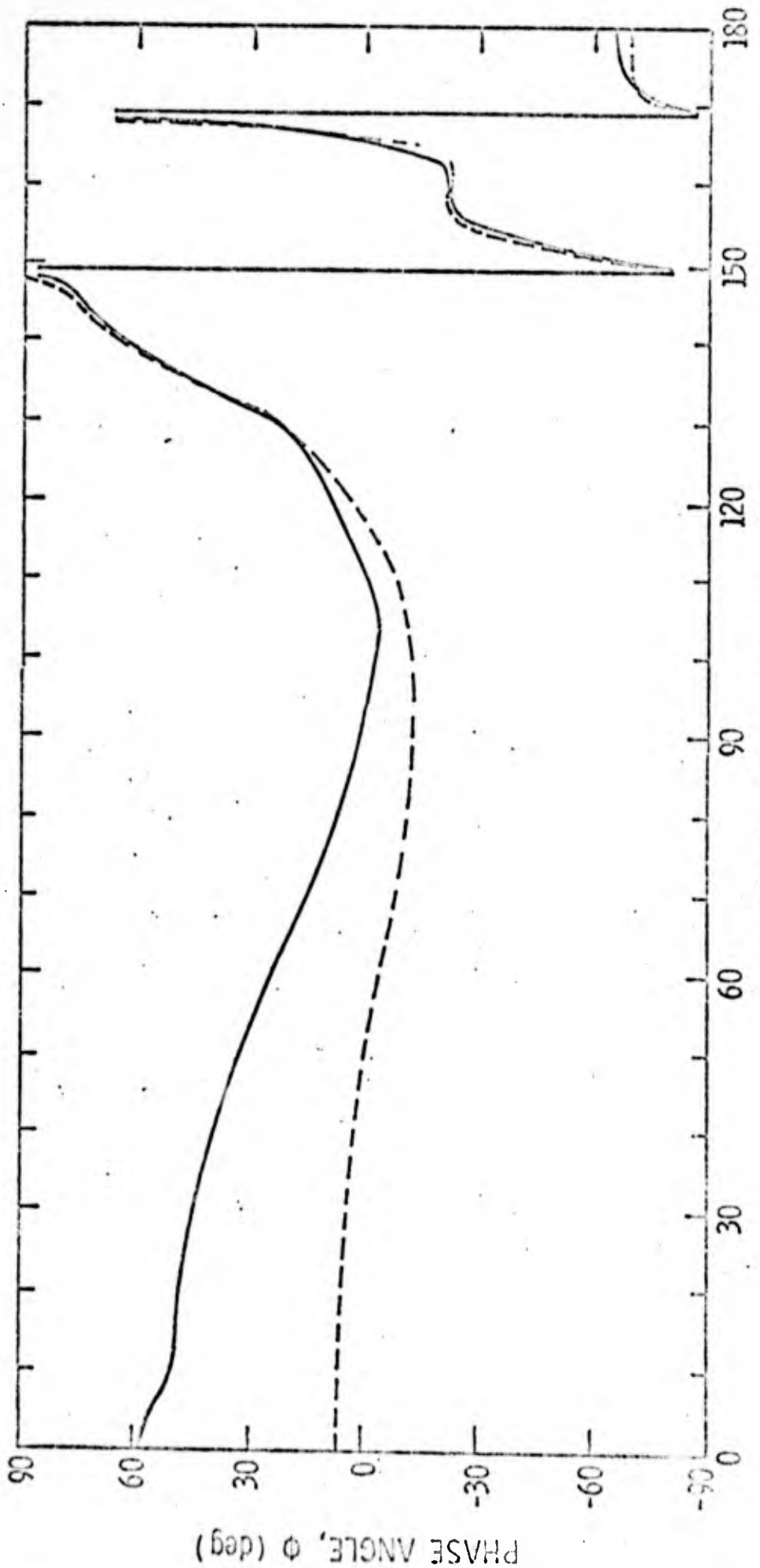

Fig. 10. Phase angle relative to incident field as a function of aspect angle for aluminum shell with ka = 10.0, 2h/a = 7.8125 x 10^{-3}, r_o/a = 1.125, ——— in air, and - - - - in water.

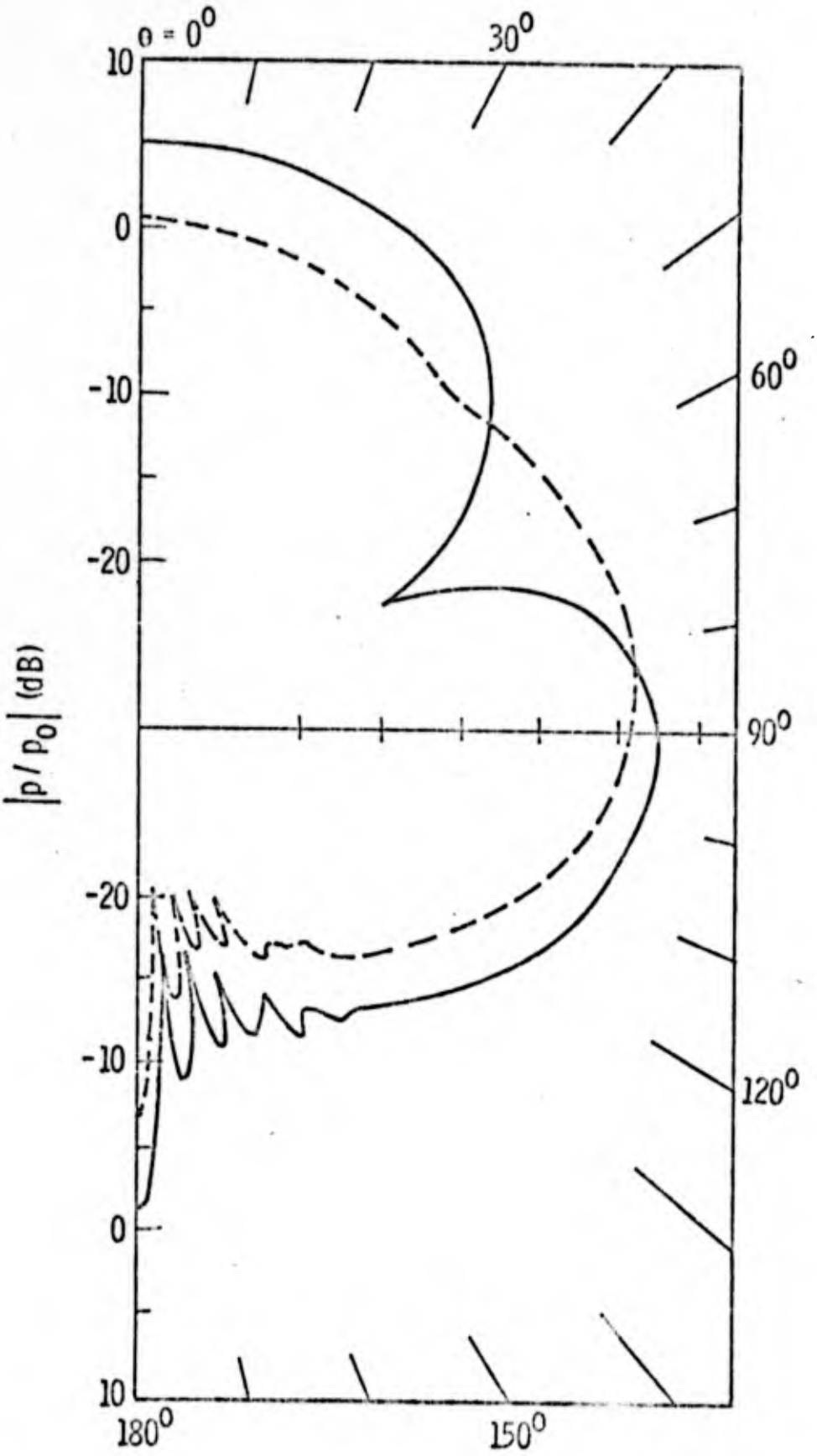

Fig. 11. Directivity function for aluminum shell with ka = 25.0, 2h/a = 7.5 x 10^{-3}, r_o/a = 1.125, ——— in air, and - - - - in water.